14th International Symposium on the Packaging and Transportation of Radioactive Materials (PATRAM 2004), Berlin, Germany, September 20-24, 2004

Paper # 169

Performance of the improved version of Monte Carlo Code A^{3}MCNP for cask shielding design

Y. Miyake[*], M. Ohmura, T. Hasegawa[1], K. Ueki[2], O. Sato[3], A. Haghighat, G. E. Sjoden[4]

1) Mitsubishi Heavy Industries, Yokohama 220-8401, Japan
2) Tokai University, Kanagawa 259-1292, Japan
3) Mitsubishi Research Institute, Tokyo 100-8141, Japan
4) Department of Nuclear and Radiological Engineering, University of Florida, Gainesville, FL 32611, USA

Abstract

A^{3}MCNP (Automatic Adjoint Accelerated MCNP) is a revised version of the MCNP Monte Carlo code, that automatically prepares variance reduction parameters for the CADIS (Consistent Adjoint Driven Importance Sampling) methodology. Using a deterministic "importance" (or adjoint) function, CADIS performs source and transport biasing within the weight-window technique. The current version of A^{3}MCNP uses the 3-D Sn transport TORT code to determine a 3-D importance function distribution. Based on simulation of several real-life problems, it is demonstrated that A^{3}MCNP provides precise calculation results with a remarkably short computation time by using the proper and objective variance reduction parameters. However, since the first version of A^{3}MCNP provided only a point source configuration option for large-scale shielding problems, such as spent-fuel transport casks, a large amount of memory may be necessary to store enough points to properly represent the source. Hence, we have developed an improved version of A^{3}MCNP (referred to as A^{3}MCNPV) which has a volumetric source configuration option. This paper describes the successful use of A^{3}MCNPV for cask neutron and gamma-ray shielding problem.

KEY WORDS: radiation shielding, Monte Carlo, MCNP, A^{3}MCNP, A^{3}MCNPV

I. Introduction

A^{3}MCNP (Automatic Adjoint Accelerated MCNP) [1] is a revised version of Monte Carlo code, MCNP, which automatically prepares variance reduction parameters for the CADIS (Consistent Adjoint Driven Importance Sampling) methodology. Using a deterministic "importance" (adjoint) function, CADIS performs source and transport biasing within the weight-window technique. The current version of A^{3}MCNP uses the 3-D Sn transport TORT code [2] to determine a 3-D importance function distribution. A^{3}MCNP provides precise calculation results with remarkably short calculation times using the proper objective variance reduction parameters.[3]

Several shielding benchmark analyses by A^{3}MCNP have been reported which show excellent agreement with measured results.[4]-[5] However, since the original A^{3}MCNP version provides only a point source distribution configuration option, large-scale shielding problems, such as spent-fuel transport casks, can require a large amount of computer memory. Hence, an improved version of A^{3}MCNP (referred to as A^{3}MCNPV) have incorporated an option for volumetric source configurations. A^{3}MCNPV shows excellent performance for neutron and gamma-ray shielding calculations of concrete cask. [8]-[9]

This paper shows the performance of A^{3}MCNPV for shielding calculations of concrete cask and of metal cask, and demonstrates the applicability of A^{3}MCNPV for an actual cask shielding problem.

II. Methodology

1. A^{3}MCNP methodology

A^{3}MCNP uses the CADIS (Consistent Adjoint Driven Importance Sampling) methodology [3], which performs source and transport biasing with the MCNP's weight-window technique.

The formulation for the source biasing is given by

$$\hat{q}(p) = \frac{\psi^+(p)q(p)}{\int_p \psi^+(p)q(p)dp} \qquad (1)$$

where $\psi^+(p)$ is the importance function at phase space $p(=\vec{r}, E, \hat{\Omega})$, where $q(p)$ is the "unbiased" source distribution, and $\hat{q}(p)$ is the biased source. To conserve the original number of source particles, the particle weight is modified using the following formulation

$$W(p) = \frac{R}{\psi^+(p)} \qquad (2)$$

where R is the total detector response which equals to the denominator of Eq. 1.

For transport biasing, A^{3}MCNP simulates the particle transport between events in the normal way, and alters the number of particles emerging in p from an event in p' by the ratio of the importances ($\psi^+(p)/\psi^+(p')$). This means that if the ratio is > 1, particles are split, while if the ratio is < 1, particles are processed through a game of Russian roulette. To preserve the expected number of particles, the particle statistical weight following the transport from p' to p is modified according to

$$W(p) = W(p') \left[\frac{\psi^+(p')}{\psi^+(p)} \right] \qquad (3)$$

A^{3}MCNP utilizes Eqs. 1 and 2 for calculating source biasing parameters, and Eq. 3 for transport biasing.

A^{3}MCNP performs the following major tasks:

(a) Generates a mesh distribution for the deterministic Sn calculation based on the MCNP defined geometry.
(b) Prepares an input file for the TORT Sn code.
(c) Prepares an input file for the GIP code [6] for generation of multi-group cross sections.
(d) Runs GIP and TORT codes, and determines a space- and energy-dependent importance function distribution

(e) Prepares a biased source $\hat{q}(\vec{r}, E)$

(f) Calculates space- and energy-dependent weight-window lower bounds (W_l) as

$$W_\ell(r,E) = \frac{R}{\phi^+(r,E)} \cdot \frac{1}{\left(\dfrac{C_u + 1}{2}\right)}$$

where ϕ^+ is the scalar adjoint function, Cu=Wu/W_l (implemented in MCNP) is the ratio of upper and lower weight window values.

(g) Superimposes the deterministic Sn spatial-mesh distribution and energy-group structure onto the Monte Carlo model in a "transparent" manner;
(h) Updates the particle weight, as each particle is transported through the "transparent" mesh.

The flowchart shown in Fig.1 presents the steps performed in an A^{3}MCNP simulation.
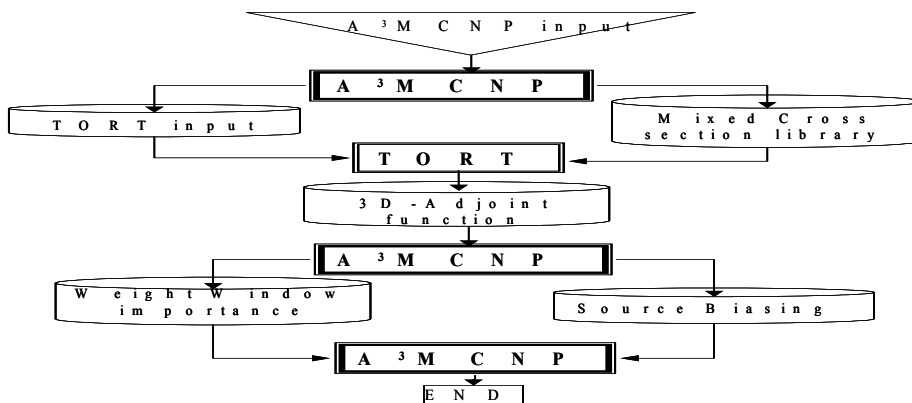

Fig. 1 Flowchart of A^{3}MCNP calculation

2. Improved methodology

The MCNP code offers various options for modeling a source distribution. The original version of A³MCNP can only prepare a biased source if the source is represented as a point-wise distribution. This means that if the unbiased source distribution were volumetric, then it had to be replaced by an equivalent point-wise distribution. Although this procedure was automated using an independent point source generation code rendering approximations to volumetric source definitions, this limitation may result in the need for large amount of computer memory if a problem includes a source which is distributed over large segments of the volume.

To overcome this limitation, a new algorithm has been implemented into A³MCNPV for automatic preparation of a biased volumetric source distribution. Since the importance function is determined in a multigroup form, depending on the form of the original MCNP source spectrum, A³MCNPV uses different formulations. If the source spectrum is in a histogram form, the biased source is given by

$$\hat{q}_{cell,g} = \frac{\overline{\phi}^{+}_{cell,g} q_{cell} \chi_g}{R} \qquad (4)$$

where, g refers to energy group g, 'cell' refers to the combinatorial MCNP cell, $\overline{\phi}^{+}_{cell,g}$ is the average "importance" function calculated over a MCNP cell, q_{cell} is the unbiased cell-wise source value, X_g is the original source spectrum. If the source spectrum is in the form of a continuous function, then the same unbiased spectrum is used for all cells. This means that Eq. 4 is rewritten as

$$\hat{q}_{cell,g} = \frac{\widetilde{\phi}^{+}_{cell} q_{cell} \chi_g}{R} \qquad (5)$$

where $\widetilde{\phi}^{+}_{cell}$ is the average "importance" function calculated over each cell and summed over all energy groups.

III. Results and discussion
1. Concrete cask shielding problem

The calculation model of the concrete cask is shown in Fig.2, which has a cylindrical configuration of approximately 400 cm in diameter, and 600 cm in height, and contains twenty-one PWR spent fuel assemblies.

The neutron dose along the ventilation duct of the upper part of the cask (referred to as streaming points) is calculated using point detector estimators, and the neutron dose along the radial surface of the cask (referred to as penetrating points) is calculated using ring detector estimators. Both calculations use the ENDF-B/VI [7] cross section library. Source neutrons are generated from the accumulated actinides in the spent fuel assemblies through spontaneous fission and (α, n) reactions. The fuel assemblies are sub-divided into a central fuel part and a structural part; both ends are homogenized accordingly to model the source region. The TORT adjoint source is placed around the cask surface at the duct exit level for streaming points and at the outer region of the cask surface for penetrating points. The conversion factor (flux- to- dose) is used as the energy spectrum multiplier.

The gamma-ray dose from both fission products and activation products is calculated at the streaming points and at the penetrating points. The estimator and the TORT adjoint source are same as those of the neutron dose except for an additional calculation case of activation products. Source gamma-rays from the fission products are generated in the spent fuel assemblies with a most probable energy spanning from 0.5 to 1 MeV. Source gamma-rays from the activation products, mainly Co-60 are generated in the both ends of the fuel assemblies (=structural parts) with energy of 1.17 and 1.33 MeV.

Neutron dose calculation results of A³MCNPV compared with those of MCNP are shown in Table 1 and 2. The weight-window technique is employed for variance reduction for the MCNP calculation. The computational cost of the TORT adjoint calculation of A³MCNPV is generally low because the methodology does not necessarily require a highly accurate adjoint flux over the spatial-mesh. The coarse spatial-mesh size $\Delta x=\Delta y=\Delta z=20$ cm is adopted for the A³MCNPV calculation. Computational efficiency is represented by the figures of merit (FOM), defined as $1/((FSD)^2 x(computation\ time))$. Table 1 provides ratios of FOMs computed between A³MCNPV and MCNP; these

range from 12 to 47 at the streaming points. Table 2 shows similar FOM ratios; these range from 5 to 35 for the penetrating points, emphasizing the clear advantage of the accelerated adjoint methodology for the cask problem.

Gamma-ray dose calculation results of A^{3}MCNPV compared with those of MCNP are also shown in Tables 1 and 2. Gamma-ray dose calculations require the consideration of spatial-mesh size tuning for the TORT adjoint calculation because gamma-rays attenuate so rapidly that a finer spatial-mesh is necessary in heavy materials (iron etc.) compared with light materials (concrete etc.). A^{3}MCNPV has an option of back-thinning, where the maximum mesh thickness is established for each material. The option is adopted as the maximum mesh size 0.5 cm for iron (concrete lining region).

Table 1 shows the FOM ratios between A^{3}MCNPV and MCNP ranging from 1.1 to 27 for fission products gamma-rays, from 0.3 to 18 for activation products gamma-rays at the streaming points, and Table 2 shows the FOM ratios from 1.7 to 10 for fission products gamma-rays, from 0.4 to 2.3 for activation gamma-rays at the penetrating points.

As the FOM ratios of activation gamma-rays are generally lower than those of fission products gamma-rays, another calculation is executed for activation gamma-rays at the streaming points with the more refined input conditions: maximum mesh size 0.1 cm for iron of back-thinning option and adjoint source placed at the duct exit. Table 1 shows that the FOM ratios of this calculation from 2.2 to 140 are larger than the former calculation remarkably. It is likely that the more limited leakage path for activation gamma-rays compared with that of fission products gamma-rays requires the more refined setting of input conditions.

2. Metal cask shielding problem

The calculation model of the metal cask is shown in Fig.3, which has a cylindrical configuration of approximately 250 cm in diameter, and 600 cm in height, and contains twenty-one PWR spent fuel assemblies.

The neutron dose along the radial surface of the cask is calculated using ring detector estimators. Source neutrons are generated from the accumulated actinides in the spent fuel assemblies through spontaneous fission and (α, n) reactions. The fuel assemblies are sub-divided into a central fuel part and a structural part; both ends are homogenized accordingly to model the source region. The TORT adjoint source is placed at the outer region of the cask radial surface. The conversion factor (flux- to- dose) is used as the energy spectrum multiplier.

The gamma-ray dose from fission products is calculated at the same points of the neutron dose. The estimator and the TORT adjoint source are same as those of the neutron dose. Source gamma-rays from the fission products are generated in the spent fuel assemblies with a most probable energy spanning from 0.5 to 1 MeV.

Neutron dose calculation results of A^{3}MCNPV compared with those of MCNP are shown in Table 3. The weight-window technique is employed for variance reduction for the MCNP calculation. The coarse spatial-mesh size $\Delta x = \Delta y = \Delta z = 20$ cm is adopted for the A^{3}MCNPV calculation. Table 3 provides ratios of FOMs computed between A^{3}MCNPV and MCNP; these range from 3.0 to 13, which are nearly equal as those for concrete cask shown in Table 2.

Gamma-ray dose calculation results of A^{3}MCNPV compared with those of MCNP are also shown in Tables 3. The back-thinning option is adopted for A^{3}MCNPV as the maximum mesh size 0.1 cm for iron. Table 3 shows the FOM ratios between A^{3}MCNPV and MCNP ranging from 1.8 to 4.4, whch are slightly lower than those for concrete cask shown in Table 2. As are mentioned in the previous chapter, gamma-ray dose calculations require the consideration of spatial-mesh size tuning in heavy materials. It is likely that metal cask requires this consideration much more than concrete cask because shielding material is composed of iron itself.
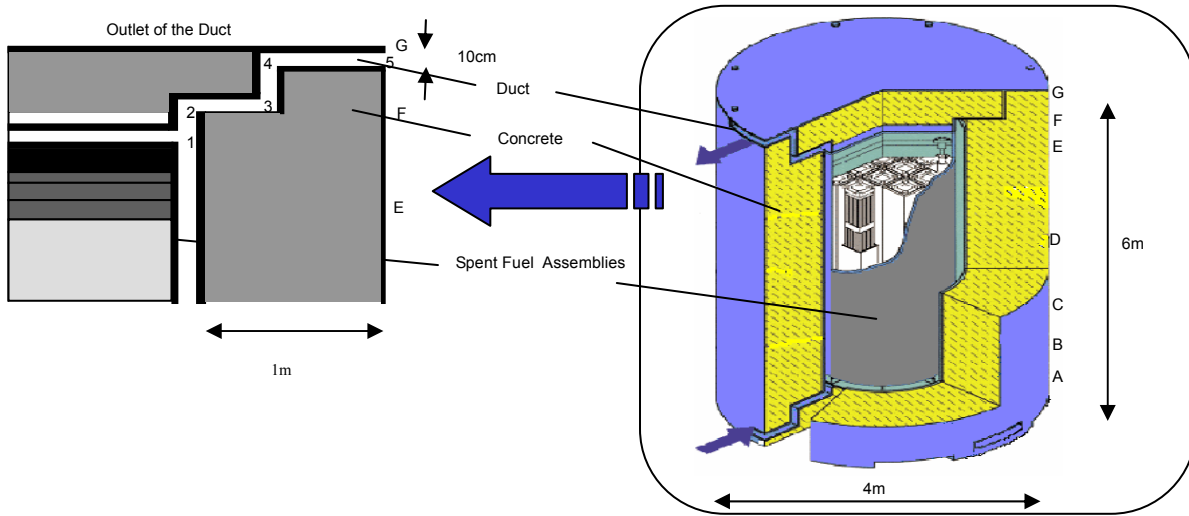
Fig. 2 Calculation model of concrete cask shielding problem

Table 1 Results of the concrete cask at the streaming points

position	Neutron		FOM ratio	Gamma-ray (Fission products)		FOM ratio
	Dose rate (µSv/h) (FSD (%))			Dose rate (µSv/h) (FSD (%))		
	A^{3}MCNPV	MCNP		A^{3}MCNPV	MCNP	
1 (entrance)	$1.0 \times 10^{+4}$ (1.4 %)	$1.0 \times 10^{+4}$ (0.7 %)	14	$7.1 \times 10^{+5}$ (0.6 %)	$5.8 \times 10^{+5}$ (3.1 %)	26
2	$4.9 \times 10^{+3}$ (2.0 %)	$4.9 \times 10^{+3}$ (0.9 %)	12	$3.6 \times 10^{+5}$ (0.8 %)	$3.5 \times 10^{+5}$ (4.2 %)	27
3	$2.9 \times 10^{+2}$ (3.4 %)	$3.2 \times 10^{+2}$ (2.5 %)	25	$9.5 \times 10^{+2}$ (3.2 %)	$9.2 \times 10^{+2}$ (6.3 %)	3.7
4	$3.0 \times 10^{+1}$ (4.5 %)	$3.4 \times 10^{+1}$ (4.2 %)	44	$7.2 \times 10^{+0}$ (3.2 %)	$7.2 \times 10^{+0}$ (4.5 %)	1.1
5 (exit)	$1.0 \times 10^{+0}$ (5.0 %)	$1.1 \times 10^{+0}$ (4.8 %)	47	3.9×10^{-2} (5.4 %)	2.7×10^{-2} (8.1 %)	2.1
Input Condition	Spatial mesh size : Δx=Δy=Δz=20cm Adjoint source : placed around the cask surface at the duct exit level			Spatial mesh size : Δx=Δy=Δz=20cm Option of back-thinning : 0.5cm for iron Adjoint source : placed around the cask surface at the duct exit level		

FSD: Fractional Standard Deviation

position	Gamma-ray (activation products)		FOM ratio			FOM ratio
	Dose rate (µSv/h) (FSD (%))			Dose rate (µSv/h) (FSD (%))		
	A^{3}MCNPV	MCNP		A^{3}MCNPV	MCNP	
1 (entrance)	$3.8 \times 10^{+5}$ (0.8 %)	$3.9 \times 10^{+5}$ (6.4 %)	18	$3.8 \times 10^{+5}$ (0.7 %)	$3.9 \times 10^{+5}$ (6.4 %)	140
2	$1.1 \times 10^{+5}$ (1.7 %)	$1.1 \times 10^{+5}$ (7.5 %)	6.0	$1.1 \times 10^{+5}$ (1.1 %)	$1.1 \times 10^{+5}$ (7.5 %)	76
3	$6.7 \times 10^{+2}$ (2.3 %)	$6.8 \times 10^{+2}$ (7.4 %)	2.8	$6.6 \times 10^{+2}$ (3.5 %)	$6.8 \times 10^{+2}$ (7.4 %)	7.0
4	$2.3 \times 10^{+1}$ (2.2 %)	$2.3 \times 10^{+1}$ (2.9 %)	0.5	$2.3 \times 10^{+1}$ (2.5 %)	$2.3 \times 10^{+1}$ (2.9 %)	2.2
5 (exit)	1.8×10^{-1} (4.9 %)	1.7×10^{-1} (5.3 %)	0.3	1.7×10^{-1} (4.0 %)	1.7×10^{-1} (5.3 %)	3.0
Input Condition	Spatial mesh size : Δx=Δy=Δz=20cm Option of back-thinning : 0.5cm for iron Adjoint source : placed around the cask surface at the duct exit level			Spatial mesh size : Δx=Δy=Δz=20cm Option of back-thinning : 0.1cm for iron Adjoint source : placed at the duct exit		

Table 2 Results of the concrete cask at the penetrating points

Position(*)	Neutron Dose rate (μ Sv/h) (FSD (%)) A³MCNPV	Neutron Dose rate (μ Sv/h) (FSD (%)) MCNP	FOM ratio	Gamma-ray (Fission products) Dose rate (μ Sv/h) (FSD (%)) A³MCNPV	Gamma-ray (Fission products) Dose rate (μ Sv/h) (FSD (%)) MCNP	FOM ratio	Gamma-ray (activation products) Dose rate (μ Sv/h) (FSD (%)) A³MCNPV	Gamma-ray (activation products) Dose rate (μ Sv/h) (FSD (%)) MCNP	FOM ratio
A (Z=-257.5cm)	7.5×10^{-1} (4.1 %)	7.8×10^{-1} (4.8 %)	14	3.8×10^{-1} (4.0 %)	3.6×10^{-1} (11 %)	10	3.6×10^{-1} (4.6 %)	3.6×10^{-1} (6.2 %)	2.3
B (Z=-242.5cm)	9.4×10^{-1} (3.4 %)	9.5×10^{-1} (3.7 %)	13	7.0×10^{-1} (5.3 %)	6.3×10^{-1} (6.3 %)	1.7	5.0×10^{-1} (4.2 %)	5.0×10^{-1} (3.2 %)	0.8
C (Z=-202.5cm)	$2.2 \times 10^{+0}$ (2.6 %)	$2.1 \times 10^{+0}$ (2.5 %)	9.9	3.9×10^{0} (1.6 %)	$3.9 \times 10^{+0}$ (3.7 %)	7.0	1.5×10^{0} (3.0 %)	$1.5 \times 10^{+0}$ (2.9 %)	1.2
D (Z= 0cm)	$7.9 \times 10^{+0}$ (1.4 %)	7.7×10^{0} (1.1 %)	6.2	$1.6 \times 10^{+1}$ (1.0 %)	$1.6 \times 10^{+1}$ (2.3 %)	6.0	4.1×10^{-3} (3.1 %)	3.9×10^{-3} (3.7 %)	1.9
E (Z=202.5cm)	$2.0 \times 10^{+0}$ (2.7 %)	$1.9 \times 10^{+0}$ (1.9 %)	5.4	3.9×10^{0} (1.8 %)	3.8×10^{0} (3.5 %)	4.8	7.4×10^{0} (1.8 %)	7.1×10^{0} (1.3 %)	0.7
F (Z=277.5cm)	2.9×10^{-1} (1.5 %)	2.8×10^{-1} (4.2 %)	7.8	8.0×10^{-2} (6.1 %)	7.4×10^{-2} (8.0 %)	2.1	3.8×10^{-1} (3.8 %)	3.9×10^{-1} (2.0 %)	0.4
G (Z=327.5cm)	2.0×10^{-1} (4.2 %)	2.2×10^{-1} (7.8 %)	35	2.1×10^{-2} (4.0 %)	2.0×10^{-2} (9.9 %)	7.2	3.1×10^{-2} (5.0 %)	3.6×10^{-2} (6.2 %)	2.1
Input Condition	Spatial mesh size : Δx=Δy=Δz=20cm Adjoint source : placed at the outer region of the cask surface			Spatial mesh size : Δx=Δy=Δz=20cm Option of back-thinning : 0.5cm for iron Adjoint source : placed at the outer region of the cask surface					

(*) The position from A to G are located at the radial surface of the cask. "Z" means the axial distance from the cask center.
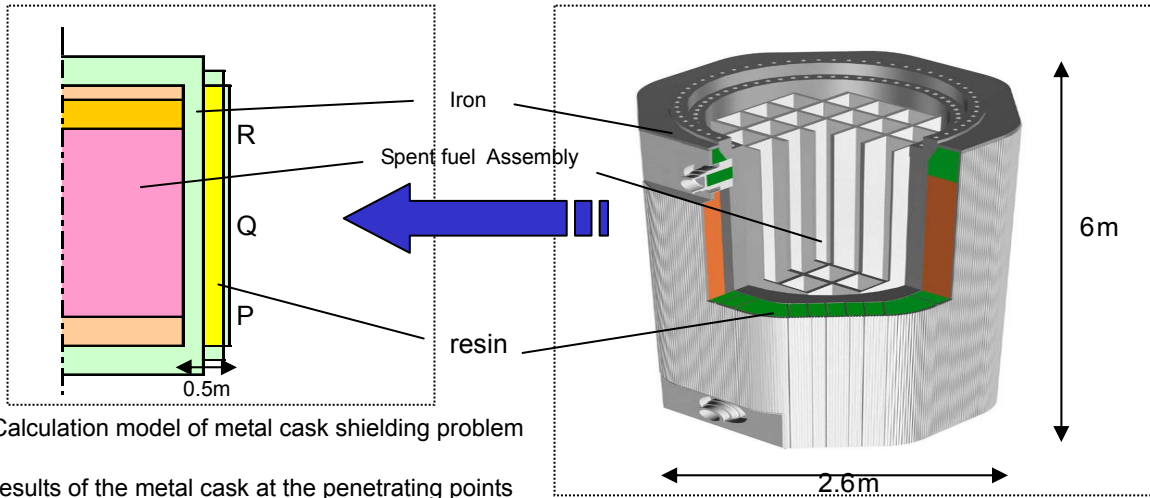

Fig. 3 Calculation model of metal cask shielding problem

Table 3 Results of the metal cask at the penetrating points

Position(*)	Neutron Dose rate (μSv/h) (FSD (%)) A³MCNPV	Neutron Dose rate (μSv/h) (FSD (%)) MCNP	FOM ratio	Gamma-ray (Fission products) Dose rate (μSv/h) (FSD (%)) A³MCNPV	Gamma-ray (Fission products) Dose rate (μSv/h) (FSD (%)) MCNP	FOM ratio
P (Z=-225cm)	$4.6 \times 10^{+0}$ (4.9 %)	$5.4 \times 10^{+0}$ (7.5 %)	3.0	$1.2 \times 10^{+1}$ (9.4 %)	$9.5 \times 10^{+0}$ (5.9 %)	1.8
Q (Z=0cm)	$3.4 \times 10^{+1}$ (1.9 %)	$3.5 \times 10^{+1}$ (3.3 %)	4.2	$1.6 \times 10^{+2}$ (2.4 %)	$1.5 \times 10^{+2}$ (2.4 %)	4.4
R (Z=200cm)	$5.8 \times 10^{+0}$ (4.0 %)	$8.6 \times 10^{+0}$ (7.1 %)	13	$4.3 \times 10^{+1}$ (5.8 %)	$4.6 \times 10^{+1}$ (5.3 %)	3.8
Input Condition	Spatial mesh size : Δx=Δy=Δz=20cm Option of back-thinning : 0.1cm for iron Adjoint source : placed at the outer region of the cask radial surface			Spatial mesh size : Δx=Δy=Δz=20cm Option of back-thinning : 0.1cm for iron Adjoint source : placed at the outer region of the cask radial surface		

(*) The position from P to R are located at the radial surface of the cask. "Z" means the axial distance from the cask center.

IV. Conclusion

We have confirmed the excellent performance of A^{3}MCNPV compared with MCNP for both the concrete cask and the metal cask shielding problem. These results lead us to the conclusion that A^{3}MCNPV is indeed an effective calculation code for large-scale shielding problems which otherwise may normally require tremendous computation times for accurate results by other calculation codes/methods. The performance of A^{3}MCNPV for neutron-induced secondary gamma-ray calculations remains as a matter to be explored in the future studies.

References

[1] Haghighat, A. and J.C. Wagner, "Monte Carlo Variance Reduction with Deterministic Importance Functions," Progress of Nuclear Energy Journal, Vol. 42 (1), Jan. 2003.

[2] Rhoades, W.A. and D.B. Simpson (1997), The TORT Three-Dimensional Discrete Ordinates Neutron/ Photon Transport Code, Oak Ridge National Laboratory, ORNL/TM-13221.

[3] Wagner, J.C. and A. Haghighat (1998), Automated Variance Reduction of Monte Carlo Shielding Calculations Using the Discrete Ordinates Adjoint Function, Nucl. Sci. Eng., 128, p. 186, 1998.

[4] Haghighat, A. and J. C. Wagner, "Application of A^{3}MCNP to Radiation Shielding Problems," Advanced Monte Carlo for Radiation Physics, Particle Transport Simulation and Applications, pp. 619-624, Springer-Verlag, 2001.

[5] Haghighat, A., H. Hiruta, and B. Petrovic, "Performance of A^{3}MCNPTM for Calculation of 3-D Neutron Flux Distribution in a BWR Core Shroud," Reactor Dosimetry Radiation Metrology and Assessment, ASTM STP 1398, pp. 549-556, Feb. 2001.

[6] Rhoades, W.A. (1978), The GIP Program for Preparation of Group-Organized Cross-Section Libraries, Informal Notes, April. Available through the Radiation Safety Information Computational Center (RSICC) as code package PSR-229, Oak Ridge, TN.

[7] Rose, P.F., "ENDF/B-VI Summary Documentation," BNL-NCS-17541 (ENDF-201), 4th Edition (October 1991).

[8] Miyake, Y. et al., "Improvement of Monte Carlo A^{3}MCNP for Large-Scale shielding Problems", Proceedings of The Second iTRS International Symposium on Radiation Safety and Detection Technology (ISORD-2), Journal of Nuclear Science and Technology Supplement 4 March 2004.

[9] Omura, M. et al., "Performance of the improved version of Monte Carlo Code A^{3}MCNP for Large-Scale shielding Problems", ICRS-RPS May 2004 (to be published).